12-15-2013

Enhanced DNA Sensing via Catalytic Aggregation of Gold Nanoparticles

Herbert M. Huttanus
Boise State University

Elton Graugnard
Boise State University

Bernard Yurke
Boise State University

William B. Knowlton
Boise State University

Wan Kuang
Boise State University

See next page for additional authors

Publication Information

Huttanus, Herbert M.; Graugnard, Elton; Yurke, Bernard; Knowlton, William B.; Kuang, Wan; Hughes, William L.; and Lee, Jeunghoon. (2013). "Enhanced DNA Sensing via Catalytic Aggregation of Gold Nanoparticles". *Biosensors and Bioelectronics, 50*, 382–386. https://doi.org/10.1016/j.bios.2013.06.063

Enhanced DNA Sensing via Catalytic Aggregation of Gold Nanoparticles

Herbert M. Huttanus
Department of Materials Science & Engineering
Boise State University
Boise, Idaho 83725, United States

Elton Graugnard
Department of Materials Science & Engineering
Boise State University
Boise, Idaho 83725, United States

Bernard Yurke
Department of Materials Science & Engineering
and
Department of Electrical & Computer Engineering
Boise State University
Boise, Idaho 83725, United States

William B. Knowlton
Department of Materials Science & Engineering
and
Department of Electrical & Computer Engineering
Boise State University
Boise, Idaho 83725, United States

Wan Kuang
Department of Electrical & Computer Engineering
Boise State University
Boise, Idaho 83725, United States

William L. Hughes
Department of Materials Science & Engineering
Boise State University
Boise, Idaho 83725, United States

and **Jeunghoon Lee**
Department of Chemistry and Biochemistry
Boise State University
Boise, Idaho 83725, United States

KEYWORDS: DNA, nanoparticle, catalytic aggregation, colorimetric detection, hybridization chain reaction

Tel: +1 208 426 3473

Fax: +1 208 426 1311

Abstract

A catalytic colorimetric detection scheme that incorporates a DNA-based hybridization chain reaction into gold nanoparticles was designed and tested. While direct aggregation forms an inter-particle linkage from only one target DNA strand, the catalytic aggregation forms multiple linkages from a single target DNA strand. Gold nanoparticles were functionalized with thiol-modified DNA strands capable of undergoing hybridization chain reactions. The changes in their absorption spectra were measured at different times and target concentrations and compared against direct aggregation. Catalytic aggregation showed a multifold increase in sensitivity at low target concentrations when compared to direct aggregation. Gel electrophoresis was performed to compare DNA hybridization reactions in catalytic and direct aggregation schemes, and the product formation was confirmed in the catalytic aggregation scheme at low levels of target concentrations. The catalytic aggregation scheme also showed high target specificity. This application of a DNA reaction network to gold nanoparticle-based colorimetric detection enables highly-sensitive, field-deployable, colorimetric readout systems capable of detecting a variety of biomolecules.

1. Introduction

Gold nanoparticle (NP)-based colorimetric detection exploits the plasmonic coupling during NP aggregation.(Elghanian et al. 1997; Ghosh and Pal 2007) Gold NPs with appropriate surface functionalization provide a simple and inexpensive method for sensing an expanding range of analytes such as nucleic acids,(Bai et al. 2010; Deng et al. 2012; Reynolds III et al. 2000; Storhoff et al. 1998) biomolecules,(Beqa et al. 2011; Fu et al. 2012; Kim et al. 2012; Wang et al. 2010; Zhao et al. 2007) organic molecules,(Ai et al. 2009) and metal ions.(Beqa et al. 2011; Chen et al. 2012; Lee et al. 2007; Lou et al. 2011; Luo et al. 2012; Xue et al. 2008) Gold NP-based detection methods have several advantages over other techniques because 1) gold NPs have high extinction coefficients, which translates to a stronger signal and high sensitivity and 2) their color change can be detected without instrumentation.(Storhoff et al. 1998) Despite these advantages, the most common methods for nucleic acid sensing remain using fluorescent dyes and polymerase chain reaction (PCR).(Lakowicz 2006; Saiki et al. 1985; Schweitzer and Kingsmore 2001; Wang et al. 2009)

Conventional gold NP-based colorimetric detection requires additional amplification steps to increase its sensitivity, undermining the simplicity of the method. To overcome these limitations and to avoid the complexity of amplification steps such as PCR, we devised a strategy to allow a single target DNA to form multiple NP linkages thus significantly increasing the detection sensitivity. Engineered DNA reaction networks based on hybridization reactions offer an option for simple amplification of DNA strands.(Zhang and Seelig 2011) For example, an entropy-driven catalytic DNA reaction network was designed to undergo cascading reactions and amplify DNA signals.(Zhang et al. 2007) Also, through hybridization chain reaction (HCR), double helix chains of variable lengths were formed from two hairpin DNA strands in the presence of an initiator strand.(Dirks and Pierce 2007; Pierce et al. 2006) The sensitivity of gold NP-based colorimetric detection can be enhanced by implementing a similar DNA reaction network because the number of target strands can be amplified by such a network. In this paper, we report the implementation of HCR for the catalytic aggregation (**CA**) of gold NPs for enhanced colorimetric detection. The **CA** design was tested and it exhibited a multifold increase in detection sensitivity as compared to the direct aggregation (**DA**) scheme which is conventionally adopted.

2. Materials and Methods

Spherical gold nanoparticles of approximately 25 nm in diameter were synthesized by the reduction of gold chloride using sodium citrate.(Turkevich et al. 1951) Briefly, 100 mL of 0.25 mM $HAuCl_4$ was heated to a boil and 1 mL of sodium citrate (0.51 mM) was added with vigorous stirring. The solution was heated for an additional 15 min and then allowed to cool to room temperature. The size of NPs was measured using transmission electron microscopy (TEM) and UV-Vis spectroscopy. Thiolated DNA strands, obtained from Integrated DNA Technologies, were first reduced using 0.1 M dithiothreitol (DTT) solution to cleave disulfide bonds, followed by an elution through a desalting column (NAP-10, GE healthcare) to remove unreacted DTT. Following quantification by absorbance measurements at 260 nm, DNA strands were mixed with gold NPs in a 500:1 ratio and the phosphate buffer concentration was increased to 10 mM and pH 7.4 along with 0.01 % (w/w) sodium dodecylsulfate (SDS). Following an overnight incubation, the NaCl concentration was gradually brought up to 0.3 M over 2 hours by additions of 4 M NaCl.(Hurst et al. 2006) The NPs were purified further by centrifugation (three times at 17200 g for 15 min) to remove any unreacted excess DNA strands. After each centrifugation, the NP pellet was re-dispersed in 10 mM phosphate buffer (pH 7.4, 0.01% (w/w) SDS, and 0.3 M NaCl) and the NP concentration was determined by measuring absorbance at 525 nm. The hybridization of target (**T**) strand to linker (**L**) strand bound to NPs was accomplished by overnight incubation of **L** strand-functionalized NPs with 500 times excess of **T** strand followed by purification by centrifugation to remove excess unreacted **T** strands.

For each aggregation reaction, three reagents - the two complementary types of functionalized NPs and the target – were mixed in a plastic cuvette sealed with paraffin film. All aggregation reactions were conducted in 10 mM phosphate buffer (pH = 7.4) with 0.3 M NaCl and 0.01% (w/w) SDS. Each 400 µL sample had a final gold NP concentration of 314 pM (157 pM of each type of NP). The **T** strand concentrations specified in the Results and Discussion section are multiples of 157 pM. Absorbances for each reaction were measured at 0, 1, 2, 4, 8, and 20 hours from the time of mixing all reagents.

Hybridization reactions of DNA strands used for gel electrophoresis were carried out in 10 mM phosphate buffer (pH 7.4), 0.01% SDS (w/w) and 0.3 M NaCl. Each hybridization reaction was allowed to sit at room temperature for 4 hours before being loaded into the gels. The gel composition was 3% agarose in 1× TAE buffer with 5 µg/mL ethidium bromide. The gels were run at 100 V for 45 min.

3. Results and Discussion

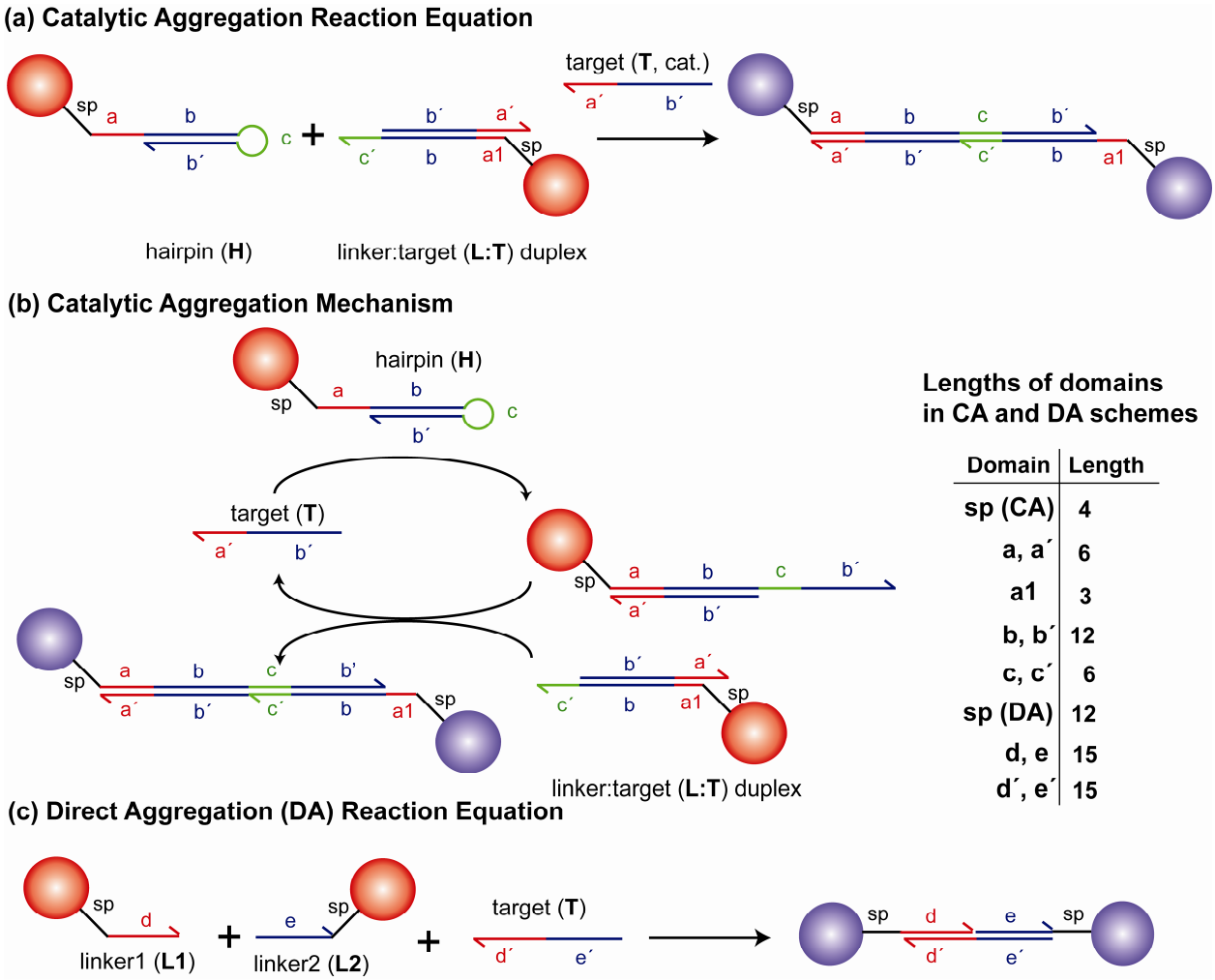

Figure 1. (a) Overall reaction equation and (b) reaction mechanism of catalytic aggregation reactions. Catalytic aggregation takes place between **H** strand-functionalized NPs and **L:T** duplex-functionalized NPs in the presence of free **T** strands. After an inter-particle linkage is formed, the **T** strand is regenerated, which propagates the reaction further (c) Overall reaction equation of conventional direct NP aggregation (complete base sequences are available in Table S1).

Catalytic aggregation (**CA**) of gold NPs provides greater detection sensitivity compared to direct aggregation (**DA**) through the formation of multiple NP linkages from a single target DNA strand. The overall reaction of the **CA** scheme is illustrated in the reaction equation of Fig. 1(a) and the reaction mechanism of Fig. 1(b). Gold NPs are functionalized with either hairpins (**H**) or linker:target (**L:T**) duplexes and aggregate only in the presence of the target (**T**) strand. This hybridization reaction can be considered as a reaction between stoichiometric amounts of **H** strand and **L:T** duplex triggered by catalytic amounts of the **T** strand forming the **H:L** product that links two NPs. Due to the catalytic nature of the reaction, one **T** strand can cause formation of multiple inter-particle linkages. As illustrated in Fig. 1(b), NP aggregation is triggered when a **T** strand linearizes an **H** strand by toehold-mediated strand displacement. In this step, the a´ domain on the **H** strand acts as the toehold for hybridization with the **T** strand.(Yurke et al. 2000; Zhang and Winfree 2009) Once in a linear configuration, the c and b´ domains of the **H** strand are exposed. In the next step, the exposed c´ domain of **L** strand acts as the toehold for another strand displacement reaction that releases the **T** strand in **L:T** duplex. Two crucial events – formation of a linkage between two NPs and the release of a **T** strand – take place in this second step. The released **T** strand can reinitiate the entire sequence of DNA reactions thus propagating and enhancing NP aggregation. As a result, multiple linkages between

NPs can form for every free **T** strand present in the system. In principle, a target DNA in a HCR network can form an unlimited number of NP linkages. Thus, the combination of a HCR network with gold NPs creates a system capable of catalytic aggregation for high-sensitivity colorimetric detection.

On the other hand, the **DA** scheme using gold NPs is composed of two different types of gold NPs, each functionalized with single-stranded DNA complementary to different parts of a target DNA strand, as illustrated in Fig. 1(c). Hybridization of both NPs to the same target effectively binds the NPs together, and the resulting NP aggregation induces a detectible change in their peak absorption magnitude and peak shift. In such conventional **DA** designs, target DNA is able to form only a single inter-particle linkage, which limits the sensitivity of this method.

The **CA** design involves a 40 nucleotide (nt) hairpin strand (**H**) and a linker (**L**, 25 nt) : target (**T**, 18 nt) duplex. The domain lengths are specified in Fig. 1 and the base sequences of all DNA strands are listed in Table S1. Instead of two hairpin strands used for the original HCR,(Pierce et al. 2006) a hairpin strand (**H**) and a duplex (**L:T**) were used to alleviate steric hindrance between NPs that arises when the more than two NPs are linked into a single DNA double helix. Also, an extra domain (a1, 3 nt) that is complementary to half of the a´ domain was included to minimize reactions between **L** strand-bound **T** strands with **H** strands by sequestering a portion of the a´ domain and provide an advantage to free **T** strands in hybridizing with **H** strands. To compare the performance of the **CA** designs against a conventional colorimetric detection scheme, a **DA** scheme was also tested. DNA strands used for the **DA** scheme are composed of 12 nt spacer (sp) and 15 nt active domains (d and e). The inter-particle distance of NP aggregates produced from DA scheme is 54 bp, which is similar to that of **CA** (47 bp).

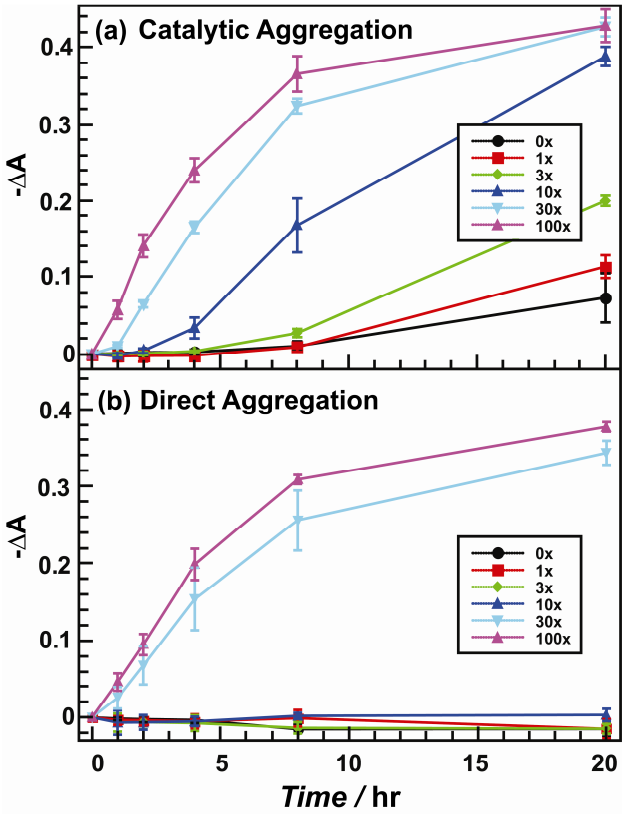

Figure 2. Absorbance change as a function of target concentration and time for (a) catalytic aggregation and (b) direct aggregation schemes. The **CA** scheme exhibits a detectable signals at 3× and 10× while **DA** scheme does not show any detectable signal at those target concentrations.

NP aggregation experiments of the **CA** scheme was conducted by adding varying amounts of target strand to a 1:1 mixture of **H** strand-functionalized NPs and **L:T** duplex-functionalized NPs. The decreases of UV-vis peak absorbance (-ΔA) and the peak shifts (Fig S2) for each sample were used as a metrics to quantify the extent of NP aggregation. The target concentrations in Fig. 2 are multiples of 157 pM (1× = 157 pM). As shown in Fig. 2(a) the **CA** scheme exhibited detectable -ΔA at low (1×, 3×, and 10×) target concentrations, whereas -ΔA from the **DA** scheme at such low target concentrations were either absent (1× and 3×) or minimal (10×). These results indicate

that measurable NP aggregation takes place even at low target DNA levels due to the catalytic nature of **CA** schemes. While the number of inter-particle linkages in **DA** scheme was not sufficient to cause detectable change in their optical properties in such low target concentrations, in the **CA** scheme, changes in optical properties are observed because more inter-particle linkages were formed for every **T** strand, hence enhancing the overall sensitivity of colorimetric detection. 1× and 10× samples in **CA** scheme exhibit similar level of -□A to 10× and 30× samples in **DA** scheme after 20 hrs, respectively. These results suggest that between three to ten-fold increase of sensitivity was achieved at those concentrations. As expected, -ΔA from **DA** samples significantly increased at higher (30× and 100×) target concentrations to levels comparable to the **CA** scheme because sufficient amounts of **T** strands were present to cause extensive NP aggregation even without **T** strand regeneration (Fig. 2(b)). The impact of higher **T** strand concentration on NP aggregation in the **CA** schemes was diminished because further aggregation induced by extra **T** strands in higher concentration had less impact on the optical properties of the NPs. The **CA** scheme exhibited slight NP aggregation even in the absence of the **T** strand, as evidenced by -ΔA in a negative control (0×) sample (Fig. 2(a)). This shift indicates that the DNA hybridization reaction can be initiated by not only free **T** strands but also by **T** strands from the **L:T** duplex. Partial protection of a´ domain by a1 domain and steric hindrance between NPs in such instances proved insufficient to completely suppress such unintended initiation.

Simulation results (Fig. S3 in supplementary materials), obtained using a domain-level strand-displacement computational system,(Phillips and Cardelli 2009) provide an insight into the difference between the **DA** and the **CA** systems. The simulations were run with 5 times excess NP-bound DNA strands (**L1** and **L2** for **DA** and **H** and **L:T** for **CA**) with respect to **T** strands, which well represents the condition at **T** strand concentrations as high as 10×, considering the large estimated number of thiol-modified DNA strands on 25-nm gold NPs.(Hurst et al. 2006) As expected, the concentration of **T** strands in **CA** scheme remains relatively stable after an initial decrease, whereas in **DA** scheme, **T** strand concentration continues to decrease because the strand is continuously being consumed as the reaction proceeds. In the **DA** scheme, the extent of the DNA hybridization reaction is limited by lower **T** strand concentration compared to concentration of NP-bound DNA strands (**L1** and **L2**). In the **CA** scheme, hybridization reactions involving **H** strands and **L:T** duplexes reach near completion because they are not limited by low **T** strand concentration and NP aggregation takes place even at **T** strand concentrations lower than 3×. At high (30× and 100×) **T** strand concentrations, the two schemes show similar kinetic behaviors. These simulation results explain the huge disparity in NP aggregation in the two schemes at low target concentrations.

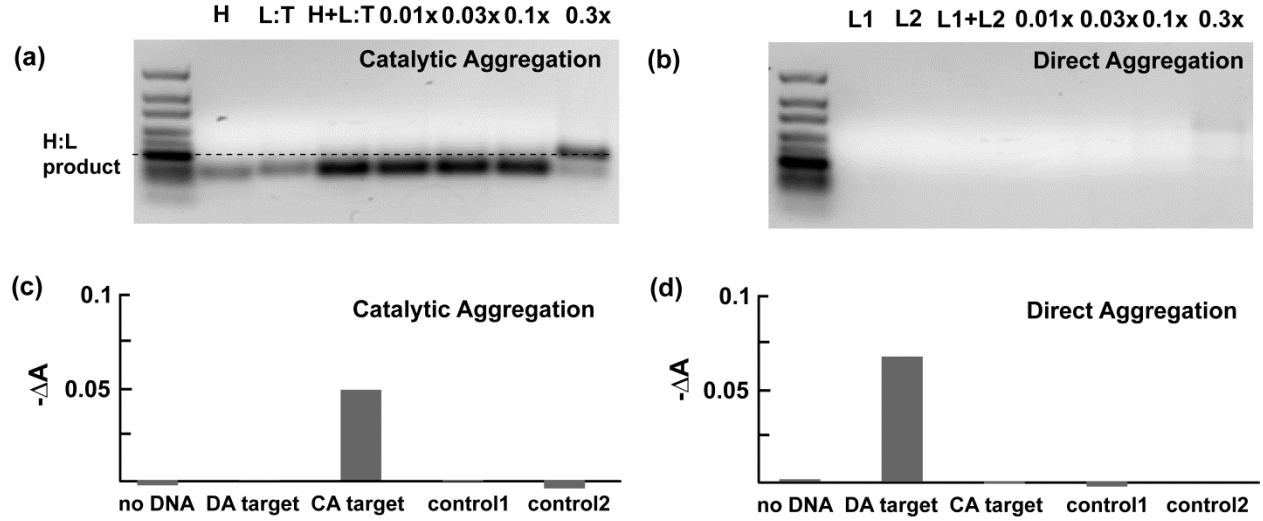

Figure 3. Agarose gel electrophoresis results of DNA strands used in (a) **CA** and (b) **DA** schemes. In the **CA** scheme, a distinct product band was observed when the **T** strand concentration was as low as 0.3×. (c,d) Absorbance decrease at 4 hrs with 30× concentration of specific and non-specific target strands. In the **CA** scheme, maximum □A values were induced by the target (**T**) strands specific to the scheme.

To verify the correct operation of the **CA** scheme, agarose gel electrophoresis of the DNA strands without NPs was performed. The DNA strands were incubated for 4 hrs prior to the electrophoresis, which was carried out in a 3% agarose gel at 100 V for 45 min. The agarose gels were stained with ethidium bromide to label double-helix bands. Two major bands were observed from the **CA** sample (Fig. 3 (a)). The lower molecular weight band (lower band) represents the mixture of **H** strands and **L:T** duplexes. The higher molecular weight band (upper band)

represents the **H:L** product that links two NPs together. In **CA** the scheme, the product band became significant at 0.3× target concentration. In the DA scheme, no appreciable double helix band was observed at low concentrations with a faint band appearing at 0.3× target concentration. These gel electrophoresis results verify that the **H:L** product, hence inter-particle linkages, formed at much lower **T** strand concentrations in the **CA** scheme.

To test target specificity, aggregation experiments of the two schemes were tested with each of four DNA strands at 30× concentrations and 4 hr reaction times (Fig. 3 (c) and (d)). The four strands were **T** strands for **DA**, **CA,** and two control strands (**C1** and **C2**). The control strands were designed with random, non-specific base sequences either in the a´ or b´ domain of the **T** strand. For example, the Control 1 (**C1**) strand has the same toehold region (domain a´ in Fig. 1(b)) as the **T** strand while the rest of the sequence is not identical to the b´ domain of the **T** strand. The Control 2 (**C2**) strand has a random toehold region (a´ domain) while the b´ domain is identical to the **T** strand. In each design, the correct target strand caused the largest absorbance decrease. The peak shifts from control target strands were comparable to those exhibited by samples without target strands. These results indicate that the catalytic aggregation schemes are very specific, and the DNA strand that can both attach to the toehold and open the hairpin is necessary to initiate NP aggregation.

4. Conclusions

In conclusion, we successfully implemented a modified HCR network to induce catalytic aggregation of gold NPs with lower concentrations of target DNA strands than detectable by direct aggregation. The catalytic aggregation design exhibited a multifold increase of absorbance change at low target concentrations, indicating more extensive NP aggregation compared to the direct aggregation scheme. Our results demonstrate that DNA hybridization reaction networks can be used to induce multiple inter-particle linkages for every target strand, enhancing the sensitivity of colorimetric detection of DNA. Design improvements will enable detection of various nucleic acid targets with different lengths. We also envision that this work can be expanded using DNA aptamers for sensing biomolecules beyond nucleic acids.

Acknowledgements

The authors thank Mr. Colin Green at Micron Technology for TEM imaging. The project described was supported by: (1) the W.M. Keck Foundation, (2) NIH Grant Number K25GM093233 from the National Institute of General Medical Sciences, (3) the Mountain States Tumor & Medical Research Institute, (4) INBRE Program, NIH Grant Numbers P20RR016454 (National Center for Research Resources) and P20GM103408 (National Institute of General Medical Sciences), and (5) DARPA Contract Number N66001-01-C-80345.

References

Ai, K., Liu, Y., Lu, L., 2009. J. Am. Chem. Soc. 131, 9496-9497.
Bai, X., Shao, C., Han, X., Li, Y., Guan, Y., Deng, Z., 2010. Biosens. and Bioelectron. 25, 1984-1988.
Beqa, L., Singh, A.K., Khan, S.A., Senapati, D., Arumugam, S.R., Ray, P.C., 2011. ACS Appl. Mater. & Interfaces 3(3), 668-673.
Chen, L., Fu, X., Lu, W., Chen, L., 2012. ACS Appl. Mater. & Interfaces 2013, 284-290.
Deng, H., Xu, Y., Liu, Y., Che, Z., Guo, H., Shan, S., Sun, Y., Liu, X., Huang, K., Ma, X., Wu, Y., Liang, X.J., 2012. Anal. Chem. 84(3), 1253-1258.
Dirks, R.M., Pierce, N.A., 2007. Proc. Natl. Acad. Sci. USA 101, 15275-15278.
Elghanian, R., Storhoff, J.J., Mucic, R.C., Letsinger, R.L., Mirkin, C.A., 1997. Science 277, 1078-1080.
Fu, X., Chen, L., Li, J., Lin, M., You, H., Wang, W., 2012. Biosens. and Bioelectron. 34, 227-231.
Ghosh, S.K., Pal, T., 2007. Chem. Rev. 107, 4797-4862.
Hurst, S.J., Lytton-Jean, A.K.R., Mirkin, C.A., 2006. Anal. Chem. 78, 8313-8318.
Kim, Y.T., Chen, Y., Choi, J.Y., Kim, W.-J., Dae, H.-M., Jung, J., Seo, T.S., 2012. Biosens. and Bioelectron. 33, 88-94.
Lakowicz, J.R., 2006. Principles of Fluorescence Spectroscopy, 3rd ed. ed. Springer, New York.
Lee, J.-S., Han, M.S., Mirkin, C.A., 2007. Angew. Chem. Int. Ed. 46, 4093-4096.
Lou, T., Chen, L., Chen, Z., Wang, Y., Chen, L., Li, J., 2011. ACS Appl. Mater. & Interfaces 3, 4215-4220.
Luo, Y., Zhang, Y., Xu, L., Wang, L., Wen, G., Liang, A., Jiang, Z., 2012. Analyst 137, 1866-1871.
Phillips, A., Cardelli, L., 2009. J. R. Soc. Interface 6, S419-S436. http://lepton.research.microsoft.com/webdna. Used with permission from Microsoft
Pierce, N.A., Dirks, R.M., Padilla, J.E., 2006, US patent 2006/0234261 A1.
Reynolds III, R.A., Mirkin, C.A., Letsinger, R.L., 2000. J. Am. Chem. Soc. 122, 3795-3796.
Saiki, R.K., Scharf, S., Faloona, F., Mullis, K.B., Horn, G.T., Erlich, H.A., Arnheim, N., 1985. Science 230, 1350-1354.
Schweitzer, B., Kingsmore, S., 2001. Curr. Opin. Biotechnol. 12(1), 21-27.
Storhoff, J.J., Elghanian, R., Mucic, R.C., Mirkin, C.A., Letsinger, R.L., 1998. J. Am. Chem. Soc. 120, 1949-1964.
Turkevich, J., Stevenson, P.C., Hillier, J., 1951. Discuss. Faraday. Soc. 11, 55-75.
Wang, G., Wang, Y., Chen, L., Choo, J., 2010. Biosens. and Bioelectron. 25, 1859-1868.
Wang, K., Tang, Z., Yang, C.J., Kim, Y., Fang, X., Li, W., Wu, Y., Medley, C.D., Cao, Z., Li, J., Colon, P., Lin, H., Tang, W., 2009. Angew. Chem. Int. Ed. 48(5), 856-870.
Xue, X., Wang, F., Liu, X., 2008. J. Am. Chem. Soc. 130, 3244-3245.
Yurke, B., Turberfield, A.J., Mills, A.P., Simmel, F.C., Neumann, J.L., 2000. Nature 406, 605-608.
Zhang, D.Y., Seelig, G., 2011. Nat. Chem. 3, 103-113.
Zhang, D.Y., Turberfield, A.J., Yurke, B., Winfree, E., 2007. Science 318, 1121-1125.
Zhang, D.Y., Winfree, E., 2009. J. Am. Chem. Soc. 131, 17303-17314.
Zhao, W., Chiuman, W., Lam, J.C.F., Brook, M.A., Li, Y., 2007. Chem. Comm., 3729-3731.